IEEE Access
Multidisciplinary : Rapid Review : Open Access Journal

Received May 25, 2020, accepted June 16, 2020, date of publication June 25, 2020, date of current version July 6, 2020.

Digital Object Identifier 10.1109/ACCESS.2020.3004843

Energy-Efficiency for IoT System With Cache-Enabled Fixed-Wing UAV Relay

KANG SONG[1,2], (Member, IEEE), JIFA ZHANG[1], ZHENGXIA JI[1], JING JIANG[2], (Member, IEEE), AND CHUNGUO LI[3], (Senior Member, IEEE)

[1]College of Electronic and Information Engineering, Qingdao University, Qingdao 266071, China
[2]Shaanxi Key Laboratory of Information Communication Network and Security, Xi'an University of Posts and Telecommunications, Xi'an 710121, China
[3]School of Information Science and Engineering, Southeast University, Nanjing 210096, China

Corresponding author: Kang Song (sk@qdu.edu.cn)

This work was supported in part by the National Natural Science Foundation of China under Grant 61901241, Grant 61941115, Grant 61671144, Grant 61871321, and Grant 61801257, in part by the Shandong Provincial Natural Science Foundation, China, under Grant ZR2017BF028 and Grant ZR2019BF001, and in part by the Open Research Funds of Shaanxi Key Laboratory of Information Communication Network and Security under Grant ICNS201903.

ABSTRACT This paper studies the energy efficiency (EE) maximization problem of fixed-wing Unmanned aerial vehicles (UAVs) enabled Internet of Things (IoT) system, where an UAV is employed as an aerial relay with enough cache capacity to amplify and forward (AF) received signals between narrow band (NB)-IoT device and eNodeB. This paper optimizes the unconstrained trajectory of the UAV to maximize the EE of UAV-enabled IoT system to achieve the green communication. Due to the objective function is a fraction and is non-convex, it's hard to solve the optimization problem. Therefore, this paper alternately optimizes trajectory in source subspace and destination subspace with the other fixed and comes up with an algorithm based on successive convex approximation (SCA) method and Dinkelbach method to obtain a local optimal solution. Numerical results show that the proposed UAV trajectory design method can obtain much bigger EE than the running track (RT) trajectory and circular trajectory. Besides, the proposed cache-enabled AF strategy can obtain much bigger EE than non cache-enabled AF strategy.

INDEX TERMS Energy efficiency, relays, the Internet of Things (IoT), unmanned aerial vehicles, successive convex approximation.

I. INTRODUCTION

As an emerging network technology and industrial model, the Internet of Things has received extensive attention [1]–[5]. Besides, with the development of science and technology, UAVs are getting smaller and smaller and have been used in more and more civilian and military fields, especially in wireless communication systems and IoT systems [6]. What's more, UAVs have been employed as aerial base stations (BSs) and aerial relaying [7], because UAVs have many advantages over unmanned ground vehicles (UGVs), such as high mobility, fast networking and flexible deployment [8]. For instance, the UAVs have been efficiently used for IoT communication [9]. Besides, the UAVs can be employed as BSs to provide mobile users with lots of data [10]. Due to the high mobility, UAVs can be employed to set up emergency communication systems in many disaster areas [11] and be deployed in many areas when communication in the ground is unaccessible [12]. How to make full use of the advantages of UAVs to improve the UAV-enabled wireless communication system's performance has aroused the interest of numerous relevant engineers and professionals.

According to the differences of structures, UAVs are divided into rotary-wing UAVs and fixed-wing UAVs, and different kinds of UAVs can be deployed in different communication systems. The authors in [13] studied the UAV-based wirelessly powered communication networks (WPCNs), where the UAV was employed to provide ground nodes (GNs) with a durable power supply through wireless links. The authors in [14] regarded the UAV as an aerial BS and aimed to maximize both the average throughput and the successful transmission probability. In [15], the authors focused on the UAV-to-network (U2N) and UAV-to-UAV (U2U) communications, and came up with a collaborative UAV

The associate editor coordinating the review of this manuscript and approving it for publication was Jun Wu.

sense-and-send scheme to enable the UAV-to-X communications. In [16], the authors viewed multiple UAVs as aerial BSs, and optimized the deployment of UAVs to maximize the total coverage area. The authors in [17] studied the communication between UAV and GNs in presence of Rician fading. In [18], the authors regarded the UAV as a mobile relay, and optimized the relay transmission power, source transmission power and relay trajectory to maximize communication throughput. In [19], UAVs were employed as an aerial BS to process the tasks migrated from the terminal devices (TDs). The authors in [20] came up with an EE maximization strategy for UAV swarm-enabled cell networks. In [21], the authors studied the use of network-connected UAV communications. The authors in [22] aimed to maximize the throughput of a disaster area UAV communication network by optimizing the position of the UAV. In [23], the authors studied the UAV-enabled non-orthogonal multiple access (NOMA) and aimed to maximize the sum rate by jointly optimizing the precoding and UAV trajectory. In [24], the authors studied the multiple UAVs relay enabled network in the IoT. The authors in [25] studied UAV-enabled backscatter communication (BackCom) networks and UAV was employed as a mobile relay in cognitive network [26].

However, the airborne energy of UAVs is very limited, which greatly limits the wide application of UAVs. Therefore, energy efficiency has become an increasingly important indicator in designing the UAV-enabled wireless communication systems. And how to increase EE while meeting the requirement of wireless communication systems is the focus of many researchers.

The authors in [27] came up with the running track (RT) trajectory of a fixed-wing UAV to study UAV-enabled relaying system. The authors in [28] employed the UAV to collect data from GN and studied the tradeoff between the GN and UAV. Prior work [29] regarded the UAV as a new mobile user in cellar networks and jointly optimized UAV transmission power and trajectory to maximize the average achievable rate. The energy minimization of rotary-wing UAV in UAV-enabled wireless communication was studied in [30]. The authors in [31] employed an UAV as an aerial BS to serve multiple wireless sensor nodes (SNs) and aimed to maximize the system EE. The authors in [32] employed the fixed-wing UAVs to broaden the horizon of mobile crowd sensing (MSC) and studied the UAV-enabled MSC. In [33], the authors employed a fixed-wing UAV unequipped with cache to maximize the end-to-end throughput of AF relaying system. However, the energy efficiency of UAV-enabled AF relaying in the IoT system has not been studied, which motivates this paper's work.

This paper studies the cache-enabled AF mode in UAV-enabled IoT system, which has become more and more important and has many applications [34]–[37]. The fixed-wing UAV is employed as an aerial relaying with enough cache capacity between NB-IoT device and eNodeB. The UAV buffers the received signal from NB-IoT device for a fixed time and forwards it to eNodeB in amplified-and-forward mode. The objective is to maximize the EE of the UAV-enabled IoT system, which is defined as the total communication throughput normalized by system energy consumption, and the UAV trajectory subjects to the initial position, final position and maximum velocity constrains. The cache-enabled amplified-and-forward mode in UAV-enabled IoT system has not yet been presented before. The contributions of this paper are summarized as below.

- This paper establishes the transmission model for the UAV-enabled IoT system, where the signal-to-noise ratio (SNR) and throughput are both functions of the UAV trajectory in the source subspace and destination subspace. Based on the transmission model, the formula for SNR at the receiver and throughput of cache-enabled UAV relay assisted IoT system are derived.
- This paper proposes a novel forwarding strategy that the UAV caches received signals from NB-IoT device (S) when flies in the source subspace and forwards cached signals to the eNodeB (D) when flies in the destination subspace in order to improve the SNR at the receiver of eNodeB (D). That is the UAV buffers the received signal from NB-IoT device for a fixed time and forwards it to eNodeB in amplified-and-forward mode. What's more, this paper considers unconstrained UAV trajectory optimization, which only has fixed initial and final position, to maximize energy efficiency of UAV-enabled IoT system.
- This paper comes up with an efficient algorithm to obtain a local optimal solution based on alternating optimization, fractional programming and SCA. A large number of numerical results are given to verify the analysis results. The proposed novel UAV trajectory design can obtain much bigger EE of UAV-enabled IoT system than RT trajectory and the circular trajectory. Besides, the proposed cache-enabled AF strategy can achieve much bigger EE than non-cache enabled AF strategy.

The rest of this paper is organized as below. In section II, the UAV-enabled IoT system model is introduced and the optimization problem is formulated. Iterative algorithms for solving the optimization problem are proposed in section III. Simulation results are presented in section IV, and finally this paper is concluded in section V.

II. SYSTEM MODEL

In this paper, we consider the UAV-enabled IoT system where the UAV is employed as an aerial amplified-and-forward relay with enough cache capacity. As is shown in Fig. 1, the system is made of a fixed-wing UAV, eNodeB (D) and NB-IoT device (S). And every of the UAV, eNodeB and NB-IoT device is equipped with an antenna. It's assumed that there are no communication links between D and S due to long distance or blockage on the ground. We aim to employ the UAV as an aerial relay to establish communication links between S and D in order to upload the data from S to D. We consider more general UAV flight trajectories

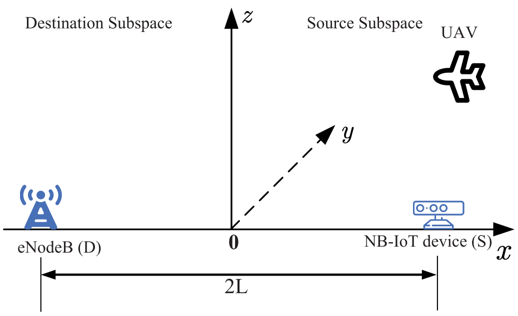

FIGURE 1. UAV-enabled IoT System Model.

design rather than fixed trajectories. To simplify the model, we divide the space into two subspaces, one subspace is the source subspace, and the other is the destination subspace. It's assumed the UAV only receives information bits from S in the source subspace and only forwards information bits to D in the destination subspace. Without loss of generality, we assume the distance between S and D is $2L$, the horizontal coordinate of S and D is $\boldsymbol{w_s} = [L, 0]^T$ and $\boldsymbol{w_d} = [-L, 0]^T$, respectively. The UAV is assumed to fly at the lowest safe flight altitude H in order to provide better wireless channel conditions. $T = 2T_1$ denotes the required mission completion time, and $\boldsymbol{q}(t) \in \mathbb{R}^{2\times 1}$ denotes the horizontal coordinate of the UAV trajectory in the source subspace, $t \in [0, T_1]$, where $\mathbb{R}$ denotes the set of all real numbers. And $\boldsymbol{k}(t) \in \mathbb{R}^{2\times 1}$ denotes the horizontal coordinate of the UAV trajectory in the destination subspace, $t \in [T_1, T]$. Let $\boldsymbol{q}_I$ and $\boldsymbol{q}_F$ denote the horizontal coordinate of original and final trajectory in the source subspace, respectively. Let $\boldsymbol{k}_I$ and $\boldsymbol{k}_F$ denote the horizontal coordinate of original and final trajectory in the destination subspace, respectively. What's more, $V_{\max}$ denotes the maximum velocity of the UAV.

The mission period T is equally discretized into $2N$ time slots which are denoted by $\delta_t = \frac{T}{2N}$. And N is chosen to be large enough so that we can assume the position of UAV is constant at every time slot. Thus, let $\boldsymbol{q}[n] = (x_1[n], y_1[n])^T$ denotes the horizontal coordinate of the UAV position in the source subspace at time slot $n \in \mathbb{N}_1 \triangleq \{1, 2, \cdots, N\}$, where $\mathbb{N}_1$ denotes a set containing all time slots when the UAV flies in the source subspace. $\boldsymbol{k}[n] = (x_2[n], y_2[n])^T$ denotes the horizontal coordinate of the UAV position in the destination subspace at time slot $n \in \mathbb{N}_2 \triangleq \{1, 2, \cdots, N\}$, where $\mathbb{N}_2$ denotes a set containing all time slots when the UAV flies in the destination subspace. As a result, the constraints on the fixed-wing UAV trajectory can be formulated as below.

$$\boldsymbol{q}[0] = \boldsymbol{q}_I, \tag{1}$$

$$\boldsymbol{q}[N] = \boldsymbol{q}_F, \tag{2}$$

$$\|\boldsymbol{q}[n] - \boldsymbol{q}[n-1]\|^2 \leqslant V^2, \quad \forall n \in \mathbb{N}_1, \tag{3}$$

$$\boldsymbol{k}[0] = \boldsymbol{k}_I, \tag{4}$$

$$\boldsymbol{k}[N] = \boldsymbol{k}_F, \tag{5}$$

$$\|\boldsymbol{k}[n] - \boldsymbol{k}[n-1]\|^2 \leqslant V^2, \quad \forall n \in \mathbb{N}_2, \tag{6}$$

where $V \triangleq V_{\max}\delta_t$ denotes the maximum flight distance of UAV at every time slot and $\|\cdot\|$ denotes the Euclidean norm. Furthermore, in Cartesian coordinates, the distance between the S and UAV at time slot $n \in \mathbb{N}_1$ can be formulated as

$$d_{s,r}[n] = \sqrt{H^2 + \|\boldsymbol{q}[n] - \boldsymbol{w}_s\|^2}, \tag{7}$$

Besides, in Cartesian coordinates, the distance between the D and UAV at time slot $n \in \mathbb{N}_2$ can be formulated as

$$d_{r,d}[n] = \sqrt{H^2 + \|\boldsymbol{k}[n] - \boldsymbol{w}_d\|^2}. \tag{8}$$

The channels between IoT nodes and UAV are assumed to be Line of Sight (LoS) channels [28]. Furthermore, we assume that the receivers of the UAV and IoT nodes can perfectly compensate the Doppler frequency shift [38]. Therefore, the channel gain from the S to UAV at time slot $n \in \mathbb{N}_1$ can be expressed as [25]

$$|h_{s,r}[n]|^2 = \frac{\beta_0}{H^2 + \|\boldsymbol{q}[n] - \boldsymbol{w}_s\|^2}, \tag{9}$$

where β_0 denotes the power gain at the distance of 1m. And the channel gain from the UAV to D at time slot $n \in \mathbb{N}_2$ can be formulated as [25]

$$|h_{r,d}[n]|^2 = \frac{\beta_0}{H^2 + \|\boldsymbol{k}[n] - \boldsymbol{w}_d\|^2}. \tag{10}$$

We assume the data is uploaded by S with constant transmission power P_s when the UAV collects data in the source subspace. The signal received by the UAV at time slot $n \in \mathbb{N}_1$ can be formulated as [39]

$$y_{s,r}[n] = \sqrt{P_s} h_{s,r}[n] x[n] + n_{s,r}[n], \tag{11}$$

where $x[n]$ denotes the signal sent by the S at time slot $n \in \mathbb{N}_1$, which is assumed to follow an independent circularly symmetric complex Gaussian distribution with unit variance and zero mean, i.e., $x[n] \sim \mathcal{CN}(0, 1)$. Besides, $n_{s,r}[n] \sim \mathcal{CN}(0, \sigma_r^2)$, where $\sigma_r^2 = N_0$ denotes noise power at the receiver of the UAV.

We assume the fixed-wing UAV has enough caching capability. The UAV caches received signals from NB-IoT device (S) when flies in the source subspace and forwards cached signals to the eNodeB (D) when flies in the destination subspace to improve the worst SNR at the receiver of D. The UAV forwards the signal received at time slot $n \in \mathbb{N}_1$ to D at time slot $n \in \mathbb{N}_2$ rather than ferries information bits in an AF manner at every time slot. That is the UAV buffers the received signal from NB-IoT device for a fixed time (T_1) and forwards it to eNodeB in amplified-and-forward mode. Therefore, the UAV amplifies the received signal at time slot $n \in \mathbb{N}_2$. The amplified signal $y_{AF}[n]$ can be formulated as [40]

$$y_{AF}[n] = \beta[n] y_{s,r}[n], \tag{12}$$

where $\beta[n] \triangleq \sqrt{\frac{P_r}{P_s|h_{s,r}[n]|^2 + N_0}}$ denotes the magnification of the transmitter of the UAV and N_0 denotes noise power at the receiver of the UAV.

Therefore, the signal received by D at time slot $n \in \mathbb{N}_2$ can be expressed as

$$\begin{aligned} z[n] &= \sqrt{P_r} h_{r,d}[n] y_{AF}[n] + n_{r,d}[n] \\ &= \sqrt{P_r} h_{r,d}[n] \sqrt{\frac{P_r}{P_s|h_{s,r}[n]|^2 + N_0}} \sqrt{P_s} h_{s,r}[n] x[n] \\ &\quad + \sqrt{P_r} h_{r,d}[n] \sqrt{\frac{P_r}{P_s|h_{s,r}[n]|^2 + N_0}} n_{s,r}[n] + n_{r,d}[n], \end{aligned} \tag{13}$$

where P_r denotes transmission power of the UAV. Besides, $n_{r,d}[n] \sim \mathcal{CN}\left(0, \sigma_d^2\right)$, where $\sigma_d^2 = N_0$ denotes noise power at the receiver of the D. Since $P_s|h_{s,r}[n]|^2 \gg N_0$, $z[n]$ can be approximated as

$$z[n] = P_r h_{r,d}[n] x[n] + \frac{P_r}{\sqrt{P_s}} \frac{h_{r,d}[n]}{h_{s,r}[n]} n_{s,r}[n] + n_{r,d}[n]. \tag{14}$$

Thus, the SNR at the receiver of D at time slot $n \in \mathbb{N}_2$ can be formulated as

$$\begin{aligned} SNR[n] &= \frac{E\left[|P_r h_{r,d}[n]|^2\right]}{E\left[|\frac{P_r}{\sqrt{P_s}} \frac{h_{r,d}[n]}{h_{s,r}[n]} n_{s,r}[n] + n_{r,d}[n]|^2\right]} \\ &\overset{(a)}{=} \frac{P_r^2 h_{r,d}^2[n]}{\frac{P_r^2}{P_s} \frac{h_{r,d}^2[n]}{h_{s,r}^2[n]} \sigma_r^2 + \sigma_d^2} \\ &\overset{(b)}{=} \frac{P_r^2 P_s h_{r,d}^2[n] h_{s,r}^2[n]}{P_r^2 h_{r,d}^2[n] \sigma_r^2 + P_s h_{s,r}^2[n] \sigma_d^2}, \end{aligned} \tag{15}$$

where $E[X]$ denotes the mathematical expectation of X. The second equation holds in (15) due to $n_{s,r}[n] \sim \mathcal{CN}\left(0, \sigma_r^2\right)$ and $n_{r,d}[n] \sim \mathcal{CN}\left(0, \sigma_d^2\right)$. Besides, the third equation holds in (15) because of simplifying the second equation holds in (15).

The instantaneous transmission rate of S at time slot n can be expressed as

$$R[n] = \log_2(1 + SNR[n]). \tag{16}$$

Thus, the sum of information bits received by D can be formulated as

$$Q = \sum_{n=1}^{N} B\delta_t \log_2(1 + SNR[n]), \tag{17}$$

where B denotes the bandwidth of relaying system.

It's obvious that the throughput Q is a function of both $\{\boldsymbol{k}[n]\}$ and $\{\boldsymbol{q}[n]\}$.

Due to N is large enough, it can be assumed that the velocity of UAV in the source subspace at each time slot $n \in \mathbb{N}_1$ is constant, which can be formulated as

$$\bar{v}_s[n] = \frac{\|\boldsymbol{q}[n] - \boldsymbol{q}[n-1]\|}{\delta_t}. \tag{18}$$

Besides, it can be assumed that the velocity of UAV in the destination subspace at each time slot $n \in \mathbb{N}_2$ is constant too, which can be formulated as

$$\bar{v}_d[n] = \frac{\|\boldsymbol{k}[n] - \boldsymbol{k}[n-1]\|}{\delta_t}. \tag{19}$$

Besides, the energy consumption of the fixed-wing UAV is made of two parts. One part is the propulsion energy used for supporting UAV's flying, the other part is the energy used for modulation, demodulation and so on. To simplify the model, we ignore the energy used for communication, for which is much less than the propulsion energy. When the fixed-wing UAV flies in the source subspace, its propulsion energy consumption can be formulated as [41]

$$\begin{aligned} \overline{E}_1 &= \sum_{n \in \mathbb{N}_1} E_s[n] + \Delta k_s \\ &= \sum_{n \in \mathbb{N}_1} \left(c_1 \frac{\bar{v}_s^3[n]}{\delta_t^2} + \frac{c_2 \delta_t^2}{\bar{v}_s[n]} \right) + \Delta k_s, \end{aligned} \tag{20}$$

where $\Delta k_s \triangleq \frac{m\left(\|\bar{v}_s[N]\|^2 - \|\bar{v}_s[1]\|^2\right)}{2}$ denotes the kinetic energy change of the UAV. c_1 and c_2 are the parameters depending on the aircraft's weight, wing area, air density and so on. And m denotes the mass of the fixed-wing UAV.

And when the fixed-wing UAV flies in the destination subspace, its propulsion energy consumption can be formulated as [41]

$$\begin{aligned} \overline{E}_2 &= \sum_{n \in \mathbb{N}_2} E_d[n] + \Delta k_d \\ &= \sum_{n \in \mathbb{N}_2} \left(c_1 \frac{\bar{v}_d^3[n]}{\delta_t^2} + \frac{c_2 \delta_t^2}{\bar{v}_d[n]} \right) + \Delta k_d, \end{aligned} \tag{21}$$

where $\Delta k_d \triangleq \frac{m\left(\|\bar{v}_d[N]\|^2 - \|\bar{v}_d[1]\|^2\right)}{2}$ denotes the kinetic energy change of the UAV.

Furthermore, the sum of energy consumed by S to complete data transmission and the energy consumed by D to download the data from the UAV can be formulated as

$$\begin{aligned} \overline{E} &= \overline{E_3} + \overline{E_4} \\ &= \sum_{n \in \mathbb{N}_1} \delta_t (P_{c1} + P_s) + \sum_{n \in \mathbb{N}_2} \delta_t P_{c2}, \end{aligned} \tag{22}$$

where P_{c1} and P_{c2} are the rated circuit power of the S and D, respectively [42].

Our objective is to maximize the EE of the IoT system by optimizing the fixed-wing UAV trajectory, subject to the UAV maximum velocity constraints, the original and final positions constraints. Therefore, the optimization problem is formulated as

$$(P1) \max_{\{\boldsymbol{k}[n], \boldsymbol{q}[n]\}} U(\boldsymbol{k}[n], \boldsymbol{q}[n]) = \frac{Q(\boldsymbol{k}[n], \boldsymbol{q}[n])}{\overline{E_1}(\boldsymbol{q}[n]) + \overline{E_2}(\boldsymbol{k}[n]) + \overline{E}} \tag{23}$$

$$\boldsymbol{k}[0] = \boldsymbol{k}_I, \tag{24}$$

$$\boldsymbol{k}[N] = \boldsymbol{k}_F, \tag{25}$$

$$\boldsymbol{q}[0] = \boldsymbol{q}_I, \tag{26}$$

$$\boldsymbol{q}[N] = \boldsymbol{q}_F, \tag{27}$$

$$\frac{\|\boldsymbol{q}[n] - \boldsymbol{q}[n-1]\|^2}{\delta_t^2} \leqslant V^2, \quad \forall n \in \mathbb{N}_1, \tag{28}$$

$$\frac{\|\boldsymbol{k}[n]-\boldsymbol{k}[n-1]\|^2}{\delta_t^2} \leqslant V^2, \quad \forall n \in \mathbb{N}_2, \tag{29}$$

III. SOLUTION OF THE OPTIMIZATION PROBLEM

Since it's difficult to optimize both $\{\boldsymbol{k}[n]\}$ and $\{\boldsymbol{q}[n]\}$, we adopt the method of alternating optimization, which alternately fixes one of $\{\boldsymbol{q}[n]\}$ and $\{\boldsymbol{k}[n]\}$ to optimize another, to gain a local optimal solution to (P1).

The objective function (23) is a complicated fraction and is non-convex. According to fractional programming theory, we adopt Dinkelbach method to solve this kind of optimization problem [43]. At first, objective function of (P1) is converted into a subtractive form by introducing a parameter η. Then, the optimization problem can be formulated as

$$\begin{aligned}(P2)\,\Gamma(\eta) = \max_{\substack{\{\boldsymbol{q}[n]\}\in\Phi_1\\ \{\boldsymbol{k}[n]\}\in\Phi_2}} & Q(\boldsymbol{k}[n],\boldsymbol{q}[n]) \\ & -\eta\left(\overline{E_1}(\boldsymbol{q}[n])+\overline{E_2}(\boldsymbol{k}[n])+\overline{E}\right) \\ & \text{s.t. } (24)\ (25)\ (26)\ (27)\ (28)\ (29).\end{aligned} \tag{30}$$

where Φ_1 and Φ_2 are the feasible set of $\{\boldsymbol{q}[n]\}$ and $\{\boldsymbol{k}[n]\}$, respectively. Besides, $\eta \geq 0$.

A. TRAJECTORY OPTIMIZATION IN THE DESTINATION SUBSPACE UNDER GIVEN TRAJECTORY IN THE SOURCE SUBSPACE

At first, we aim to optimize trajectory $\{\boldsymbol{k}[n]\}$ under given UAV trajectory $\{\boldsymbol{q}[n]\}$. Therefore the optimization problem (P2) is only related to the UAV trajectory $\{\boldsymbol{k}[n]\}$, which can be formulated as

$$\begin{aligned}(P3)\ \Gamma(\eta) = \max_{\{\boldsymbol{k}[n]\}\in\Phi_2} & Q(\boldsymbol{k}[n]) \\ & -\eta\left(\overline{E_1}+\overline{E_2}(\boldsymbol{k}[n])+\overline{E}\right) \\ & \text{s.t. } (24)\ (25)\ (29).\end{aligned} \tag{31}$$

Note that problem (P3) is a non-convex optimization problem, since the objective function is non-convex with respect to $\boldsymbol{k}[n]$. In order to solve this non-convex optimization problem, we introduce two important lemmas at first.

Lemma 1: Given c_1, c_2, δ_t, the function $\phi(\alpha) \triangleq [\frac{c_1\alpha^3}{\delta_t^2} + \frac{c_2\delta_t^2}{\alpha}]$ is convex w.r.t. $\alpha > 0$.

Proof: The second-order derivatives of $\phi(\alpha)$ w.r.t. α can be formulated as

$$\frac{\partial^2\phi(\alpha)}{\partial\alpha^2} = \frac{6c_1\alpha}{\delta_t^2} + \frac{2c_2\delta_t^2}{\alpha^3}. \tag{32}$$

We can prove that $\frac{\partial^2\phi(\alpha)}{\partial\alpha^2} > 0$ for $\alpha > 0$. Therefore, $\phi(\alpha)$ is a convex function. ■

According to Lemma 1, it is easy to prove that $E_d(\boldsymbol{k}[n])$ is a convex function w.r.t. $\|\boldsymbol{k}[n]-\boldsymbol{k}[n-1]\|$. However, $E_d(\boldsymbol{k}[n])$ is a non-convex function w.r.t. $\boldsymbol{k}[n]$ and $\boldsymbol{k}[n-1]$, respectively. SCA method can be used to derive its convex approximation [27]. Let $\{\boldsymbol{k}^{(0)}[n]\}$ denotes the original trajectory of the UAV and $\{\boldsymbol{k}^{(j)}[n]\}$ denotes the gained trajectory of the UAV at $(j-1)$-th iteration. Under any given $\{\boldsymbol{k}^{(j)}[n]\}, j \geq 0$, we can make use of the first-order Taylor approximation of $E_d(\boldsymbol{k}[n])$ to obtain its low bound, which is formulated as below.

$$E_d(\boldsymbol{k}[n]) \geqslant E_d^{lb}(\boldsymbol{k}[n]), \tag{33}$$

where $E_d^{lb}(\boldsymbol{k}[n])$ is formulated as below

$$\begin{aligned}E_d^{lb}(\boldsymbol{k}[n]) &= c_1\frac{\|\delta_n(\boldsymbol{k}^{(j)}[n])\|^3}{\delta_t^2} + \frac{c_2\delta_t^2}{\|\delta_n(\boldsymbol{k}^{(j)}[n])\|} \\ &+ \left(\frac{3c_1\|\delta_n(\boldsymbol{k}^{(j)}[n])\|^2}{\delta_t^2} - \frac{c_2\delta_t^2}{\|\delta_n(\boldsymbol{k}^{(j)}[n])\|^2}\right) \\ &\times(\|\delta_n(\boldsymbol{k}[n])\| - \|\boldsymbol{k}^{(j)}[n]\|),\end{aligned} \tag{34}$$

$\delta_n(\boldsymbol{a}[n]) = \boldsymbol{a}[n]-\boldsymbol{a}[n-1]$ and the equality in (33) is true when $\boldsymbol{k}[n] = \boldsymbol{k}^{(j)}[n]$.

Lemma 2: Given $a \triangleq P_r^2P_sh_{r,d}^2[n]\beta_0$, $b \triangleq P_r^2N_0h_{r,d}^2[n]$, $c \triangleq P_sN_0\beta_0$, the function $\xi(\rho) = \log_2(1+\frac{a}{c+b\rho})$ is convex w.r.t. ρ.

Proof: The second-order derivatives of $\xi(\rho)$ w.r.t. ρ can be formulated as

$$\frac{\partial^2\xi(\rho)}{\partial\rho^2} = \frac{b^2}{\ln 2}\left(\frac{1}{(c+b\rho)^2} - \frac{1}{(c+b\rho+a)^2}\right). \tag{35}$$

We can prove that $\frac{\partial^2\xi(\rho)}{\partial\rho^2} > 0$ for $\rho > 0$. Therefore, $\xi(\rho)$ is a convex function. ■

According to Lemma 2, it is easy to prove that $R(\boldsymbol{k}[n])$ is a convex function w.r.t. $H^2 + \|\boldsymbol{k}[n]-\boldsymbol{w}_d\|^2$. However, $R(\boldsymbol{k}[n])$ is a non-convex function w.r.t. $\boldsymbol{k}[n]$. We also use the first-order Taylor approximation of $R(\boldsymbol{k}[n])$ to obtain its low bound, which is formulated as below.

$$R(\boldsymbol{k}[n]) \geq R^{lb}(\boldsymbol{k}[n]) \tag{36}$$

where $R^{lb}(\boldsymbol{k}[n])$ is expressed as (37), shown at the bottom of the page, and the equality in (36) is true when $\boldsymbol{k}[n] = \boldsymbol{k}^{(j)}[n]$.

The low bound of $Q(\boldsymbol{k}[n])$ can be formulated as

$$Q^{lb}(\boldsymbol{k}[n]) = \sum_{n=1}^{N} B\delta_t R^{lb}(\boldsymbol{k}[n]) \tag{38}$$

$$\begin{aligned}R^{lb}(\boldsymbol{k}[n]) &= \log_2\left(1+\frac{a}{b(H^2+\|\boldsymbol{k}^{(j)}[n]-\boldsymbol{w}_d\|^2)+c}\right) \\ &- \frac{\frac{a}{b}(\|\boldsymbol{k}[n]-\boldsymbol{w}_d\|^2 - \|\boldsymbol{k}^{(j)}[n]-\boldsymbol{w}_d\|^2)\log_2 e}{((H^2+\|\boldsymbol{k}^{(j)}[n]-\boldsymbol{w}_d\|^2)+\frac{c}{b})((H^2+\|\boldsymbol{k}^{(j)}[n]-\boldsymbol{w}_d\|^2)+\frac{c+a}{b})}\end{aligned} \tag{37}$$

Amending (P3) by replacing $E_d(\boldsymbol{k}[n])$ with $E_d^{lb}(\boldsymbol{k}[n])$, and replacing $Q(\boldsymbol{k}[n])$ with $Q^{lb}(\boldsymbol{k}[n])$, the optimization problem can be formulated as

$$(P4)\ \Gamma(\eta) = \max_{\{\boldsymbol{k}[n]\}\in\Phi_2} Q^{lb}(\boldsymbol{k}[n]) - \eta\left(\overline{E_1} + \sum_{n\in\mathbb{N}_2} E_d^{lb}(\boldsymbol{k}[n]) + \overline{E} + \Delta k_d\right)$$
$$\text{s.t. } (24)(25)\ (29). \tag{39}$$

Under given η, optimization problem (P4) is a convex optimization problem at every $\{\boldsymbol{k}^{(j)}[n]\}, j \geq 0$, which can be solved by standard convex optimization method. Thus, we come up with a inner-layer iteration algorithm based on SCA to solve the optimization problem (P4), and the algorithm is shown in Algorithm 1.

Algorithm 1 Algorithm Based on SCA Method for Problem (P4) Under Given η

1: Input the parameter η;
2: Set the original UAV trajectory as $\{\boldsymbol{k}^{(0)}[n]\}_{n=1}^{N}$, and $j = 0$;
3: **repeat**
4: Gain the optimal solution as $\{\boldsymbol{k}^{(j)*}[n]\}_{n=1}^{N}$ of problem (P4) by standard convex optimization techniques;
5: Iterate the trajectory as $\{\boldsymbol{k}^{(j+1)}[n]\} = \{\boldsymbol{k}^{(j)*}[n]\}, \forall n \in \mathbb{N}_2$;
6: Set $j = j + 1$;
7: **until** Reaches maximum number of iterations or the objective value of (P4) converges within a given accuracy.

Algorithm 2 Algorithm Based on Dinkelbach Method for Problem (P4)

1: Input the tolerance value ϵ;
2: Initialize $i = 1$, $\eta_i = 0$, $\left\{\boldsymbol{k}^*[\boldsymbol{n}]\right\}_{n=1}^{N}$;
3: **while** $\Gamma(\eta_i) > \epsilon$ **do**
4: Gain the solution $(\left\{\boldsymbol{k}^*[\boldsymbol{n}]\right\}_{n=1}^{N})$ of problem (P4) in the method of Algorithm 1;
5: Update $\eta_i = \frac{Q^{lb}(\boldsymbol{k}^*[n])}{\overline{E_1}+\sum_{n\in\mathbb{N}_2} E_d^{lb}(\boldsymbol{k}^*[n])+\overline{E}+\Delta k_d}$;
6: Set $i = i + 1$;
7: **end while**

According to [43], considering $\left\{\boldsymbol{k}^*[n]\right\} \in \Phi_2$ and $\eta^* = \frac{Q^{lb}(\boldsymbol{k}^*[n])}{\overline{E_1}+\sum_{n\in\mathbb{N}_2} E_d^{lb}(\boldsymbol{k}^*[n])+\overline{E}+\Delta k_d}$, and $\left\{\boldsymbol{k}^*[n]\right\}$ is the solution of optimization problem (P4) if and only if

$$\Gamma\left(\eta^*\right) = 0. \tag{40}$$

Thus, we can gain the optimal objective value by the method of searching the root of (40). The Dinkelbach method is an iterative algorithm, where η is updated in every iteration. We propose a two-layer iterative algorithm, in which the outer-layer iteration is based on the Dinkelbach method and the inner-layer iteration algorithm is based on SCA to find the optimal trajectory under given η. The specific two-layers iterative algorithm is shown in Algorithm 2.

B. TRAJECTORY OPTIMIZATION IN THE SOURCE SUBSPACE UNDER GIVEN TRAJECTORY IN THE DESTINATION SUBSPACE

Under given trajectory $\{\boldsymbol{k}[n]\}$, the optimization problem (P1) is only related to the $\{\boldsymbol{q}[n]\}$, which can be formulated as

$$(P5)\ \max_{\{\boldsymbol{q}[n]\}\in\Phi_1} U_s(\boldsymbol{q}[n]) = \frac{Q(\boldsymbol{q}[n])}{\overline{E_1}(\boldsymbol{q}[n]) + \overline{E_2} + \overline{E}}$$
$$\text{s.t. } (26)\ (27)(28). \tag{41}$$

The objective function (P5) is a complicated fraction and is non-convex. According to fractional programming theory, we adopt Dinkelbach method to solve this kind of problem. At first, the objective function of (P5) is converted into a subtractive form by introducing the parameter γ.

$$(P6)\quad \Gamma(\gamma) = \max_{\{\boldsymbol{q}[n]\}\in\Phi_1} Q(\boldsymbol{q}[n]) - \gamma\left(\overline{E_1}(\boldsymbol{q}[n]) + \overline{E_2} + \overline{E}\right)$$
$$\text{s.t. } (26)\ (27)(28). \tag{42}$$

where Φ_1 is the feasible set of $\{\boldsymbol{q}[n]\}$ and $\gamma \geqslant 0$. However the objective function of (P6) is non-convex. In order to solve this non-convex optimization problem, we introduce an important lemma at first.

Lemma 3: Given $d = P_r^2 P_s h_{s,r}^2[n]\beta_0$, $h = P_r^2 N_0 \beta_0$, $f = P_s N_0 h_{s,r}^2[n]$, the function $\psi(x) = \log_2\left(1 + \frac{d}{h+fx}\right)$ is convex w.r.t. x.

Proof: The two-order derivatives of $\psi(x)$ w.r.t. x can be formulated as

$$\frac{\partial^2\psi(x)}{\partial x^2} = \frac{f^2}{\ln 2}\left(\frac{1}{(h+fx)^2} - \frac{1}{(h+fx+d)^2}\right) \tag{43}$$

We can prove that $\frac{\partial^2\psi(x)}{\partial x^2} > 0$ for $x > 0$. Therefore, $\psi(x)$ is a convex function. ■

According to Lemma 3, it's easy to prove that $R(\boldsymbol{q}[n])$ is convex w.r.t. $\left(H^2 + \|\boldsymbol{q}[n] - \boldsymbol{w}_s\|^2\right)$. However, $R(\boldsymbol{q}[n])$ is non-convex w.r.t. $\boldsymbol{q}[n]$. SCA is employed to obtain the low bound of $R(\boldsymbol{q}[n])$, which can be formulated as below.

$$R(\boldsymbol{q}[n]) \geq R^{lb}(\boldsymbol{q}[n]) \tag{44}$$

where as (45), shown at the bottom of the next page, where $\{\boldsymbol{q}^{(0)}[n]\}$ denotes the original trajectory of the UAV and $\{\boldsymbol{q}^{(i)}[n]\}$ denotes the gained trajectory of the UAV at $(i-1)$-th iteration.

The low bound of $Q(\boldsymbol{q}[n])$ can be formulated as

$$Q(\boldsymbol{q}[n]) \geq Q^{lb}(\boldsymbol{q}[n]), \tag{46}$$

where

$$Q^{lb}(\boldsymbol{q}[n]) = \sum_{n=1}^{N} B\delta_t R^{lb}(\boldsymbol{q}[n]). \tag{47}$$

According to lemma 1, the low bound of $E_s(\boldsymbol{q}[n])$ can be formulated as

$$E_s^{lb}(\boldsymbol{q}[n]) = c_1\frac{\|\delta_n(\boldsymbol{q}^{(i)}[n])\|^3}{\delta_t^2} + \frac{c_2\delta_t^2}{\|\delta_n(\boldsymbol{q}^{(i)}[n])\|}$$

$$+\left(\frac{3c_1\|\delta_n(\boldsymbol{q}^{(i)}[n])\|^2}{\delta_t^2}-\frac{c_2\delta_t^2}{\|\delta_n(\boldsymbol{q}^{(i)}[n])\|^2}\right)\times(\|\delta_n(\boldsymbol{q}[n])\|-\|\boldsymbol{q}^{(i)}[n]\|), \tag{48}$$

where $\{\boldsymbol{q}^{(i)}[n]\}$ denotes the gained trajectory of the UAV at $(i-1)$-th iteration.

Amending (P6) by replacing $E_s(\boldsymbol{q}[n])$ with $E_s^{lb}(\boldsymbol{q}[n])$, and replacing $Q(\boldsymbol{q}[n])$ with $Q^{lb}(\boldsymbol{q}[n])$, the optimization problem can be formulated as

$$(P7)\ \Gamma(\gamma)=\max_{\{\boldsymbol{q}[n]\}\in\Phi_1} Q^{lb}(\boldsymbol{q}[n]) -\gamma\left(\sum_{n\in\mathbb{N}_1}E_s^{lb}[n]+\overline{E_2}+\overline{E}+\Delta k_s\right) \quad \text{s.t.}(26)\ (27)\ (28). \tag{49}$$

The optimization is similar to the optimization problem (P4). Therefore, iterative Algorithm 1 and Algorithm 2 can be used to solve this optimization problem.

C. ALTERNATING OPTIMIZATION

Now, this paper proposes a complete algorithm for solving optimization problem (P1) by alternating optimization. The algorithm optimizes trajectory $\{\boldsymbol{k}[n]\}$ by solving (P4) under given trajectory $\{\boldsymbol{q}[n]\}$ and optimizes trajectory $\{\boldsymbol{q}[n]\}$ by solving (P7) under given trajectory $\{\boldsymbol{k}[n]\}$ alternately. The detailed algorithm is shown in Algorithm 3.

Algorithm 3 Alternating Optimization Algorithm for Problem (P1)

1: Input the initial UAV trajectory $\{\boldsymbol{k}^{(0)}[n]\}$ and $\{\boldsymbol{q}^{(0)}[n]\}$;
2: Set $j=0$;
3: **repeat**
4: Gain the solution $\{\boldsymbol{k}^{(j+1)}[n]\}$ of optimization problem (P4) under given UAV trajectory $\{\boldsymbol{q}^{(j)}[n]\}$ and the energy efficiency η_d of the system;
5: Gain the solution $\{\boldsymbol{q}^{(j+1)}[n]\}$ of optimization problem (P7) under given UAV trajectory $\{\boldsymbol{k}^{(j)}[n]\}$ and the energy efficiency η_s of the system;
6: $j=j+1$;
7: **until** Reaches maximum number of iterations or $|\eta_s-\eta_d|<=\epsilon$.

IV. SIMULATION

In this section, a large number of numerical results are given to verify the performance of our proposed novel design with fixed-wing UAV trajectory. We set the maximum velocity of the UAV as $V_{\max}=20$m/s, and the noise power spectral density at the receiver as $n_0=-170$dBm/Hz, and $N_0=n_0B$. Besides, We set the wireless channel power gain as $\beta_0=-20$dB, the transmission power of S as $P_s=10$mW, the rated circuit power of the S as $P_{c1}=50$mW, the mass of the fixed-wing UAV as $m=50$kg, and the UAV's flight altitude as $H=100$m. Besides, we think that the horizontal position of the S is (1200m, 0m), the horizontal position of the D is (-1200m, 0m), and the horizontal position of the E is (0m, 0m). The parameters c_1 and c_2 are 9.26×10^{-4} and 2250, respectively. We set the bandwidth of the wireless channel between the UAV and IoT nodes as $B=1$ MHz. The original and final horizontal positions of UAV trajectory are (1200m, 0m) and (-1200m, 0m), respectively. We set each time slot as $\delta_t=1$s, and the total flying time as $T=240$s. Therefore, the flying time in the source subspace (T_1) is 120s and the flying time in the destination subspace (T_2) is 120s. We set the tolerance value as $\epsilon=10^{-3}$. What's more, for Algorithm 1 and Algorithm 2, we set the original flight trajectory of the fixed-wing UAV as a straight line, where the UAV flies from S to D with a constant velocity $V_1=\frac{\|q_I-q_F\|}{T}$, which is smaller than the maximum flight velocity $V_{\max}$. Besides, we set the circuit power of the D as $P_{c2}=50$mW and the transmission power of UAV as $P_r=12.5$mW.

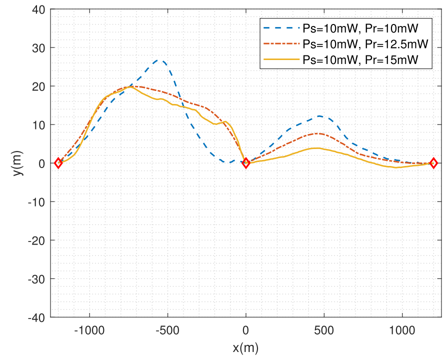

FIGURE 2. UAV trajectories versus transmission power of the NB-IoT device (S) projected onto the X-Y plane by the UAV trajectory optimization. The red diamond at the origin is the intersection of the UAV's trajectory in the source and destination subspace. The remaining two red diamonds are the initial and final positions of the UAV trajectory, respectively.

Fig. 2 shows the obtained complete UAV trajectory UAV trajectories projected onto the X-Y plane versus different transmission power of UAV, i.e., 10mW, 12.5mW and 15mW. And the energy efficiency of the UAV-enabled IoT system is 25.6kbits/Joule, 27.1kbits/Joule, 28.0kbits/Joule, respectively. As shown in the picture, the UAV flies from S to the origin (0,0) in the source subspace and from the origin (0,0) to D in the destination subspace.

$$R^{lb}(\boldsymbol{q}[n])=\log_2\left(1+\frac{d}{h(H^2+\|\boldsymbol{q}^{(i)}[n]-\boldsymbol{w}_s\|^2)}\right) -\frac{\frac{d}{h}\log_2 e(\|\boldsymbol{q}[n]-\boldsymbol{w}_s\|^2-\|\boldsymbol{q}^{(i)}[n]-\boldsymbol{w}_s\|^2)}{(\frac{d+f}{h}+(H^2+\|\boldsymbol{q}^{(i)}[n]-\boldsymbol{w}_s\|^2))((H^2+\|\boldsymbol{q}^{(i)}[n]-\boldsymbol{w}_s\|^2)+\frac{f}{h})} \tag{45}$$

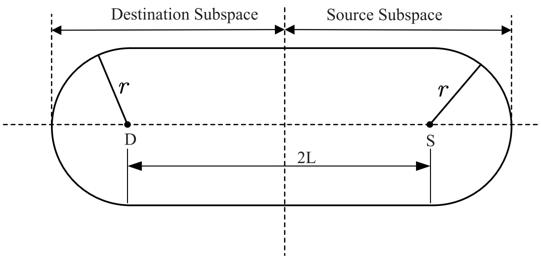

FIGURE 3. The RT trajectory relaying system.

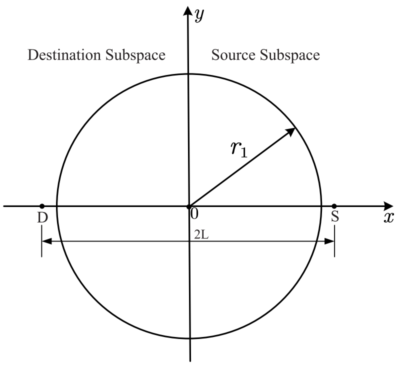

FIGURE 4. The circular trajectory relaying system.

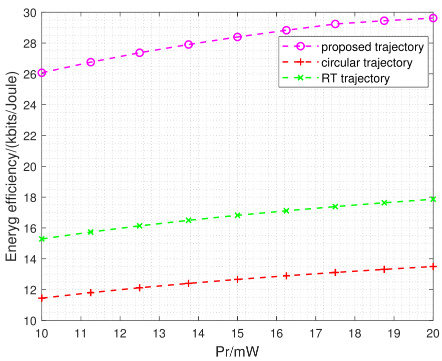

FIGURE 5. Energy efficiency of relaying system versus transmission power of the UAV.

We also introduce another two UAV trajectory designs in UAV-enabled IoT system to compare system performance. The authors in [27] came up with a RT trajectory, which is shown in Fig. 3. The RT trajectory is made of straight part and the circular part. Besides, the RT trajectory is supposed to be symmetrical for simplifying the model. The radius of the circular part is r, which is an optimization variable that needs to be optimized to maximize the EE of IoT system. Besides, the circular UAV trajectory is shown in Fig. 4, which is also supposed to be symmetrical. The radius of the circular trajectory is r_1, which is an optimization variable that needs to be optimized to maximize the EE of IoT system.

Fig. 5 shows the EE of the proposed cache-enabled UAV-enabled IoT system, RT trajectory and circular trajectory cache-enabled IoT system versus different transmission power of the UAV. It can be seen that the EE of these IoT

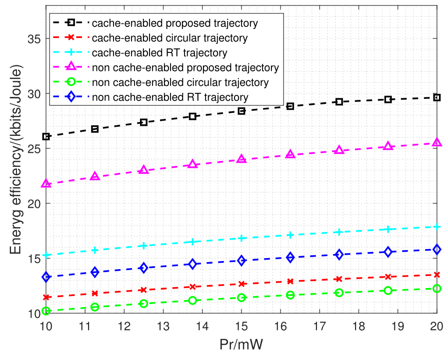

FIGURE 6. Energy efficiency of two kinds of AF strategy versus transmission power of the UAV.

systems increases with the increase of transmission power of the UAV under same transmission power of S. What's more, the EE of the proposed UAV-enabled IoT system is much bigger than that of RT trajectory and circular trajectory of UAV-enabled IoT system under the same transmission power of the UAV. Compared to the other two kinds of the UAV-enabled IoT systems, the increase of transmission power of the UAV can more greatly improve the energy efficiency of the proposed UAV-enabled IoT system.

In [33], the authors adopt another AF strategy that UAV ferries information bits in an AF manner at every time slot due to the UAV is not equipped with cache. Fig. 6 shows the energy efficiency of cache-enabled and non cache-enabled AF strategy versus transmission power of the UAV under proposed UAV trajectory, RT trajectory and circular trajectory, respectively. It can be seen that the proposed UAV-enabled IoT system obtains much bigger EE than the other two kinds of UAV-enabled IoT system, too. As can be seen from Fig. 6 that the cache-enabled AF strategy can obtain much bigger energy efficiency than non cache-enabled AF strategy, because cache-enabled AF strategy can greatly improve the SNR at the receiver of D.

V. CONCLUSION

This paper studies the fixed-wing UAV-enabled IoT system where the UAV is employed as an aerial relay with enough cache capacity to collect and forward signals between NB-IoT device and eNodeB. Besides, this paper considers a more general UAV trajectory rather than a fixed UAV trajectory, which only has fixed original position and final position. Due to the limit of the airborne energy of UAV, this paper aims to optimize the UAV trajectory to maximize the EE by using the alternating optimization, SCA technique and fractional programming theory. A large number of numerical results show that the optimized trajectory for the UAV can obtain much bigger EE when compared to the RT trajectory and the circular trajectory. Besides, the increase of transmission power of the UAV can greatly increase the energy efficiency of proposed AF relaying in the IoT system. What's more, the proposed cache-enabled AF strategy can obtain much bigger EE than non cache-enabled AF strategy. In conclusion, the proposed UAV trajectory design for the fixed-wing UAV can obtain bigger energy efficiency of the UAV-enabled IoT system.

REFERENCES

[1] H. Liang, J. Wu, S. Mumtaz, J. Li, X. Lin, and M. Wen, "MBID: Micro-blockchain-based geographical dynamic intrusion detection for V2X," *IEEE Commun. Mag.*, vol. 57, no. 10, pp. 77–83, Oct. 2019.

[2] J. Wu, M. Dong, K. Ota, J. Li, W. Yang, and M. Wang, "Fog-computing-enabled cognitive network function virtualization for an information-centric future Internet," *IEEE Commun. Mag.*, vol. 57, no. 7, pp. 48–54, Jul. 2019.

[3] J. Wu, M. Dong, K. Ota, J. Li, and Z. Guan, "FCSS: Fog-computing-based content-aware filtering for security services in information-centric social networks," *IEEE Trans. Emerg. Topics Comput.*, vol. 7, no. 4, pp. 553–564, Oct. 2019.

[4] G. Li, G. Xu, A. K. Sangaiah, J. Wu, and J. Li, "EdgeLaaS: Edge learning as a service for knowledge-centric connected healthcare," *IEEE Netw.*, vol. 33, no. 6, pp. 37–43, Nov. 2019.

[5] J. Chen, J. Wu, H. Liang, S. Mumtaz, J. Li, K. Konstantin, A. K. Bashir, and R. Nawaz, "Collaborative trust blockchain based unbiased control transfer mechanism for industrial automation," *IEEE Trans. Ind. Appl.*, early access, Dec. 13, 2019, doi: 10.1109/TIA.2019.2959550.

[6] Z. Zhou, F. Xiong, C. Xu, Z. Chang, S. Mumtaz, and J. Rodriguez, "Autonomous power line inspection based on industrial unmanned aerial vehicles: An energy efficiency perspective," in *Proc. IEEE 87th Veh. Technol. Conf. (VTC Spring)*, Jun. 2018, pp. 1–5.

[7] Y. Zeng, R. Zhang, and T. J. Lim, "Wireless communications with unmanned aerial vehicles: Opportunities and challenges," *IEEE Commun. Mag.*, vol. 54, no. 5, pp. 36–42, May 2016.

[8] S. Wang, M. Xia, K. Huang, and Y.-C. Wu, "Wirelessly powered two-way communication with nonlinear energy harvesting model: Rate regions under fixed and mobile relay," *IEEE Trans. Wireless Commun.*, vol. 16, no. 12, pp. 8190–8204, Dec. 2017.

[9] H. Dai, H. Zhang, C. Li, and B. Wang, "Efficient deployment of multiple UAVs for IoT communication in dynamic environment," *China Commun.*, vol. 17, no. 1, pp. 89–103, Jan. 2020.

[10] N. Zhao, F. Cheng, F. R. Yu, J. Tang, Y. Chen, G. Gui, and H. Sari, "Caching UAV assisted secure transmission in hyper-dense networks based on interference alignment," *IEEE Trans. Commun.*, vol. 66, no. 5, pp. 2281–2294, May 2018.

[11] N. Zhao, W. Lu, M. Sheng, Y. Chen, J. Tang, F. R. Yu, and K.-K. Wong, "UAV-assisted emergency networks in disasters," *IEEE Wireless Commun.*, vol. 26, no. 1, pp. 45–51, Feb. 2019.

[12] H. Dai, H. Zhang, M. Hua, C. Li, Y. Huang, and B. Wang, "How to deploy multiple UAVs for providing communication service in an unknown region?" *IEEE Wireless Commun. Lett.*, vol. 8, no. 4, pp. 1276–1279, Aug. 2019.

[13] H. Chen, D. Li, Y. Wang, and F. Yin, "UAV hovering strategy based on a wirelessly powered communication network," *IEEE Access*, vol. 7, pp. 3194–3205, 2019.

[14] Z. Wang, L. Duan, and R. Zhang, "Adaptive deployment for UAV-aided communication networks," *IEEE Trans. Wireless Commun.*, vol. 18, no. 9, pp. 4531–4543, Sep. 2019.

[15] S. Zhang, H. Zhang, B. Di, and L. Song, "Cellular UAV-to-X communications: Design and optimization for multi-UAV networks," *IEEE Trans. Wireless Commun.*, vol. 18, no. 2, pp. 1346–1359, Feb. 2019.

[16] M. Mozaffari, W. Saad, M. Bennis, and M. Debbah, "Efficient deployment of multiple unmanned aerial vehicles for optimal wireless coverage," *IEEE Commun. Lett.*, vol. 20, no. 8, pp. 1647–1650, Aug. 2016.

[17] M. M. Azari, F. Rosas, K.-C. Chen, and S. Pollin, "Optimal UAV positioning for terrestrial-aerial communication in presence of fading," in *Proc. IEEE Global Commun. Conf. (GLOBECOM)*, Dec. 2016, pp. 1–7.

[18] Y. Zeng, R. Zhang, and T. J. Lim, "Throughput maximization for UAV-enabled mobile relaying systems," *IEEE Trans. Commun.*, vol. 64, no. 12, pp. 4983–4996, Dec. 2016.

[19] M. Hua, Y. Wang, C. Li, Y. Huang, and L. Yang, "UAV-aided mobile edge computing systems with one by one access scheme," *IEEE Trans. Green Commun. Netw.*, vol. 3, no. 3, pp. 664–678, Sep. 2019.

[20] C. Liu, W. Feng, J. Wang, Y. Chen, and N. Ge, "Aerial small cells using coordinated multiple UAVs: An energy efficiency optimization perspective," *IEEE Access*, vol. 7, pp. 122838–122848, 2019.

[21] H. Wang, J. Wang, J. Chen, Y. Gong, and G. Ding, "Network-connected UAV communications: Potentials and challenges," *China Commun.*, vol. 15, no. 12, pp. 111–121, Dec. 2018.

[22] S. U. Rahman, G.-H. Kim, Y.-Z. Cho, and A. Khan, "Positioning of UAVs for throughput maximization in software-defined disaster area UAV communication networks," *J. Commun. Netw.*, vol. 20, no. 5, pp. 452–463, Oct. 2018.

[23] N. Zhao, X. Pang, Z. Li, Y. Chen, F. Li, Z. Ding, and M.-S. Alouini, "Joint trajectory and precoding optimization for UAV-assisted NOMA networks," *IEEE Trans. Commun.*, vol. 67, no. 5, pp. 3723–3735, May 2019.

[24] B. Ji, Y. Li, B. Zhou, C. Li, K. Song, and H. Wen, "Performance analysis of UAV relay assisted IoT communication network enhanced with energy harvesting," *IEEE Access*, vol. 7, pp. 38738–38747, 2019.

[25] M. Hua, L. Yang, C. Li, Q. Wu, and A. L. Swindlehurst, "Throughput maximization for UAV-aided backscatter communication networks," *IEEE Trans. Commun.*, vol. 68, no. 2, pp. 1254–1270, Feb. 2020.

[26] B. Ji, Y. Li, S. Chen, C. Han, C. Li, and H. Wen, "Secrecy outage analysis of UAV assisted relay and antenna selection for cognitive network under Nakagami-m channel," *IEEE Trans. Cognit. Commun. Netw.*, early access, Jan. 22, 2020, doi: 10.1109/TCCN.2020.2965945.

[27] F. Dong, L. Li, Z. Lu, Q. Pan, and W. Zheng, "Energy-efficiency for fixed-wing UAV-enabled data collection and forwarding," in *Proc. IEEE Int. Conf. Commun. Workshops (ICC Workshops)*, May 2019, pp. 1–6.

[28] D. Yang, Q. Wu, Y. Zeng, and R. Zhang, "Energy tradeoff in ground-to-UAV communication via trajectory design," *IEEE Trans. Veh. Technol.*, vol. 67, no. 7, pp. 6721–6726, Jul. 2018.

[29] Y. Huang, J. Xu, L. Qiu, and R. Zhang, "Cognitive UAV communication via joint trajectory and power control," in *Proc. IEEE 19th Int. Workshop Signal Process. Adv. Wireless Commun. (SPAWC)*, Jun. 2018, pp. 1–5.

[30] Y. Zeng, J. Xu, and R. Zhang, "Energy minimization for wireless communication with rotary-wing UAV," *IEEE Trans. Wireless Commun.*, vol. 18, no. 4, pp. 2329–2345, Apr. 2019.

[31] M. Hua, Y. Wang, Z. Zhang, C. Li, Y. Huang, and L. Yang, "Energy-efficient optimisation for UAV-aided wireless sensor networks," *IET Commun.*, vol. 13, no. 8, pp. 972–980, May 2019.

[32] Z. Zhou, J. Feng, B. Gu, B. Ai, S. Mumtaz, J. Rodriguez, and M. Guizani, "When mobile crowd sensing meets UAV: Energy-efficient task assignment and route planning," *IEEE Trans. Commun.*, vol. 66, no. 11, pp. 5526–5538, Nov. 2018.

[33] X. Jiang, Z. Wu, Z. Yin, and Z. Yang, "Power and trajectory optimization for UAV-enabled amplify-and-forward relay networks," *IEEE Access*, vol. 6, pp. 48688–48696, 2018.

[34] J. Wu, M. Dong, K. Ota, J. Li, and W. Yang, "Application-aware consensus management for software-defined intelligent blockchain in IoT," *IEEE Netw.*, vol. 34, no. 1, pp. 69–75, Jan. 2020.

[35] D. Hu, L. He, and J. Wu, "A novel forward-link multiplexed scheme in satellite-based Internet of Things," *IEEE Internet Things J.*, vol. 5, no. 2, pp. 1265–1274, Apr. 2018.

[36] J. Wu, M. Dong, K. Ota, J. Li, and Z. Guan, "Big data analysis-based secure cluster management for optimized control plane in software-defined networks," *IEEE Trans. Netw. Service Manage.*, vol. 15, no. 1, pp. 27–38, Mar. 2018.

[37] X. Lin, J. Li, J. Wu, H. Liang, and W. Yang, "Making knowledge tradable in edge-AI enabled IoT: A consortium blockchain-based efficient and incentive approach," *IEEE Trans. Ind. Informat.*, vol. 15, no. 12, pp. 6367–6378, Dec. 2019.

[38] A. Agarwal and S. K. Patra, "Receiver synchronization for digital audio broadcasting system based on phase reference symbol," in *Proc. Int. Conf. Energy, Automat. Signal*, Dec. 2011, pp. 1–6.

[39] C.-K. Tseng and S.-H. Wu, "Effective protocols and channel quality control mechanisms for cooperative ARQ with opportunistic AF relaying," *IEEE Trans. Veh. Technol.*, vol. 67, no. 3, pp. 2382–2397, Mar. 2018.

[40] M. Hua, C. Li, Y. Huang, and L. Yang, "Throughput maximization for UAV-enabled wireless power transfer in relaying system," in *Proc. 9th Int. Conf. Wireless Commun. Signal Process. (WCSP)*, Oct. 2017, pp. 1–5.

[41] Y. Zeng and R. Zhang, "Energy-efficient UAV communication with trajectory optimization," *IEEE Trans. Wireless Commun.*, vol. 16, no. 6, pp. 3747–3760, Jun. 2017.

[42] Q. Wu, G. Y. Li, W. Chen, D. W. K. Ng, and R. Schober, "An overview of sustainable green 5G networks," *IEEE Wireless Commun.*, vol. 24, no. 4, pp. 72–80, Aug. 2017.

[43] A. Zappone and E. Jorswieck. (2015). *Energy Efficiency in Wireless Networks Via Fractional Programming Theory*. [Online]. Available: https://ieeexplore.ieee.org/document/8187084

KANG SONG (Member, IEEE) received the B.S. degree from Anhui University, China, in 2009, and the Ph.D. degree in information and communication engineering from Southeast University, China, in 2016. Since August 2016, he has been a Faculty Member with the School of Electronic and Information Engineering, Qingdao University. His current research interests include cooperative communications and heterogeneous networks.

JIFA ZHANG is currently pursuing the B.S. degree with Qingdao University. His current research interests include spectrum sharing, array signal processing, and unmanned aerial vehicles communications.

ZHENGXIA JI is currently pursuing the B.S. degree with Qingdao University. Her current research interests include cooperative communications and unmanned aerial vehicles communications.

JING JIANG (Member, IEEE) received the M.Sc. degree from Xidian University, in 2005, and the Ph.D. degree in information and communication engineering from Northwestern Polytechnical University, China, in 2009. She was the Leader of 3GPP LTE MIMO project with ZTE Corporation, China, from 2006 to 2013. She is currently a Professor with the Shaanxi Key Laboratory of Information Communication Network and Security, Xi'an University of Posts and Telecommunications, Xi'an, China. Her research interests include massive multiple-input multiple-output systems and millimeter-wave communications. She was a member of 3GPP.

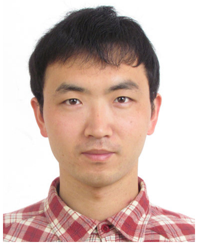

CHUNGUO LI (Senior Member, IEEE) received the bachelor's degree in wireless communications from Shandong University, in 2005, and the Ph.D. degree in wireless communications from Southeast University, Nanjing, China, in 2010.

In July 2010, he joined Southeast University, as a Faculty Member. From June 2012 to June 2013, he was a Postdoctoral Researcher with Concordia University, Montreal, QC, Canada. From July 2013 to August 2014, he was with the DSL Laboratory, Stanford University, as a Visiting Associate Professor. From August 2017 to July 2019, he was an Adjunct Professor with Xizang Minzu University, under the supporting Tibet Program organized by the China National Human Resources Ministry. He is currently an Advisor of Ph.D. candidates and a Full Professor with Southeast University. His research interests include wireless communications, cyberspace security, and machine learning-based image/video signal processing. He is a Fellow of IET. He is also the IEEE CIS Nanjing Chapter Chair.